OPEN ACCESS

TRANSLATIONAL SCIENCE

PU.1 promotes development of rheumatoid arthritis via repressing FLT3 in macrophages and fibroblast-like synoviocytes

Jiajie Tu ,[1] Weile Chen,[1] Yilong Fang,[1] Dafei Han,[1] Yizhao Chen,[1] Haifeng Jiang,[1] Xuewen Tan,[1] Zhen Xu,[1] Xuming Wu,[1] Huihui Wang,[1] Xiangling Zhu,[1] Wenming Hong,[1] Zhenbao Li,[2] Chen Zhu,[3] Xinming Wang,[1] Wei Wei [1]

Handling editor Josef S Smolen

► Additional supplemental material is published online only. To view, please visit the journal online (http://dx.doi.org/10.1136/ard-2022-222708).

[1]Institute of Clinical Pharmacology, Anhui Medical University, Hefei, China
[2]College of Pharmacy, Anhui University of Traditional Chinese Medicine, Hefei, Anhui, China
[3]Department of Orthopedics, University of Science and Technology of China, Hefei, Anhui, China

Correspondence to
Professor Wei Wei, 81# Meishan Road, Shushan District, Hefei City, Anhui Province, China; wwei@ahmu.edu.cn

JT, WC and YF contributed equally.

Received 24 April 2022
Accepted 13 September 2022
Published Online First 5 October 2022

To cite: Tu J, Chen W, Fang Y, *et al*. *Ann Rheum Dis* 2023;**82**:198–211.

ABSTRACT

Objectives To uncover the function and underlying mechanism of an essential transcriptional factor, PU.1, in the development of rheumatoid arthritis (RA).

Methods The expression and localisation of PU.1 and its potential target, FMS-like tyrosine kinase 3 (FLT3), in the synovium of patients with RA were determined by western blot and immunohistochemical (IHC) staining. UREΔ (with PU.1 knockdown) and FLT3-ITD (with FLT3 activation) mice were used to establish collagen antibody-induced arthritis (CAIA). For the in vitro study, the effects of PU.1 and FLT3 on primary macrophages and fibroblast-like synoviocytes (FLS) were investigated using siRNAs. Mechanistically, luciferase reporter assays, western blotting, FACS and IHC were conducted to show the direct regulation of PU.1 on the transcription of FLT3 in macrophages and FLS. Finally, a small molecular inhibitor of PU.1, DB2313, was used to further illustrate the therapeutic effects of DB2313 on arthritis using two in vivo models, CAIA and collagen-induced arthritis (CIA).

Results The expression of PU.1 was induced in the synovium of patients with RA when compared with that in osteoarthritis patients and normal controls. FLT3 and p-FLT3 showed opposite expression patterns compared with PU.1 in RA. The CAIA model showed that PU.1 was an activator, whereas FLT3 was a repressor, of the development of arthritis in vivo. Moreover, results from in vitro assays were consistent with the in vivo results: PU.1 promoted hyperactivation and inflammatory status of macrophages and FLS, whereas FLT3 had the opposite effects. In addition, PU.1 inhibited the transcription of FLT3 by directly binding to its promoter region. The PU.1 inhibitor DB2313 clearly alleviated the effects on arthritis development in the CAIA and CIA models.

Conclusions These results support the role of PU.1 in RA and may have therapeutic implications by directly repressing FLT3. Therefore, targeting PU.1 might be a potential therapeutic approach for RA.

WHAT IS ALREADY KNOWN ON THIS TOPIC

⇒ Rheumatoid arthritis (RA) is a common autoimmune disease that manifests primarily as arthritis. A variety of immune cells, such as T cell, B cell, macrophage and non-immune cells, such as fibroblast-like synoviocytes (FLS) and chondrocytes, are involved in the development of arthritis. PU.1 is a member of the E26 transformation-specific family of transcription factors. Previous studies have found PU.1 is critical for the differentiation of a variety of immune cells and development of several immune system-related cancers.

WHAT THIS STUDY ADDS

⇒ In the current study, we reveal for the first time the specific role and potential mechanisms of PU.1 in RA. PU.1 could promote the development of arthritis by directly targeting FMS-like tyrosine kinase 3 in both macrophage and FLS.

HOW THIS STUDY MIGHT AFFECT RESEARCH, PRACTICE OR POLICY

⇒ The specific role of PU.1 in multiple cells in RA provides new ideas and potential therapeutic targets for the pathogenesis of RA.

INTRODUCTION

Rheumatoid arthritis (RA) is a chronic inflammatory and destructive joint disease characterised by synovial hyperplasia and infiltration of different cell types into the joint synovium.[1–3] These RA-related cells can be mainly divided into two categories. The first category is considered to be the key immune cells that initiate or induce RA, including T cells, B cells, macrophages and neutrophils.[4–7] The key role of these cells in RA has been widely confirmed, which mainly reflects excessive immune activation or an inflammatory phenotype.[8 9] The other type is effector cells that receive inflammatory stimuli to further worsen RA, mainly including fibroblast-like synoviocytes (FLS)[10–12] and chondrocytes[13 14] in joints and even cells in other organs of the human body, such as fibroblasts in the lungs and heart.[15 16] These cells mainly mediate stimulating factors from the aforementioned immune cells to cause multiple levels of RA-associated damage to different organs and tissues. Therefore, the interaction between these cells is considered a key link in the pathogenesis of RA and may be a potential therapeutic target.

PU.1 is a member of the E26 transformation-specific family of transcription factors and is essential for the differentiation and function of a variety of myeloid cells.[17–19] Previous research on PU.1 has mainly focused on immune system–related

cancers.[20] The main research direction of our research group is autoimmune diseases, such as RA. This type of disease is characterised by abnormal function in a variety of immune cells.[2 3] The important role of PU.1 in these immune cells prompted us to explore its role in autoimmune diseases, especially RA. In the current study, we investigated the specific role and underlying mechanism of PU.1 in RA. Our results provide new ideas and potential therapeutic targets for the pathogenesis of RA.

RESULTS

PU.1 and FMS-like tyrosine kinase 3 expression in RA patients

To investigate the specific role of PU.1 in RA, we first determined PU.1 expression level in joint synovium from healthy donors, osteoarthritis (OA) patients and RA patients. The results of immunohistochemical (IHC) staining show that PU.1 expression in the joint synovial tissue of RA patients was upregulated compared with that of healthy donors or OA patients (figure 1A). The results of western blotting further verified the upregulation of PU.1 in the joint synovium of RA patients when compared with that of patients with OA (figure 1B). PU.1 was coexpressed with macrophages ($CD68^+$) and FLS ($Vimentin^+$) in the synovium of RA joints (figure 1C), indicating that PU.1 might exert proinflammatory effects in these two types of cells in RA. Finally, we determined PU.1 expression level in the joint synovium from a mouse collagen-induced arthritis (CIA) model. The results of IHC staining verified that PU.1 was also greatly induced in the hyperplastic joint synovium of CIA mice (figure 1D). In addition, the essential of FMS-like tyrosine

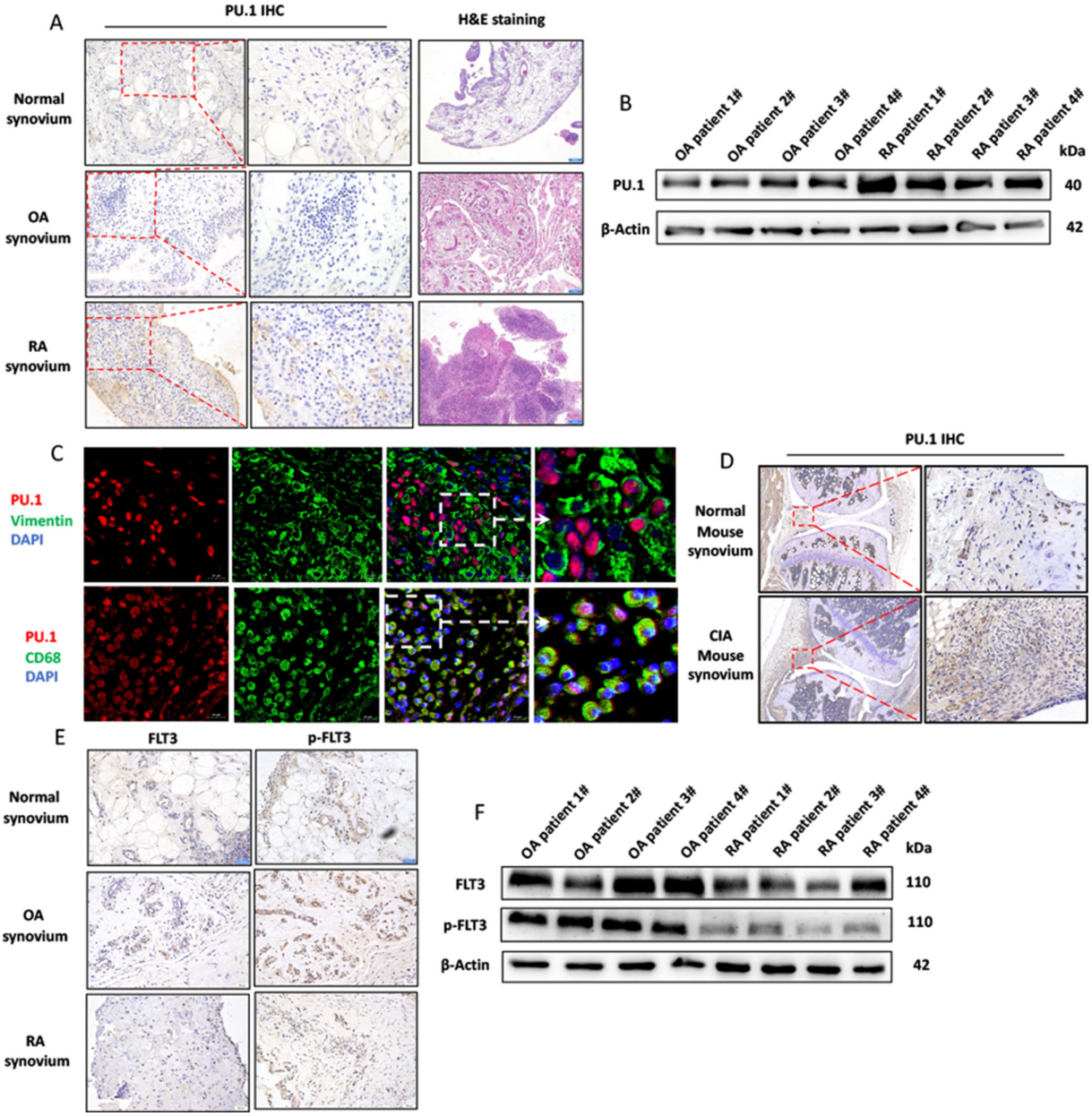

Figure 1 Expression of PU.1 and FLT3 in patients with RA. (A) IHC staining of PU.1 expression in the joint synovium of healthy donors and patients with OA and RA. (B) Western blotting results of PU.1 expression in joint synovium of patients with OA and RA. (C) Double-staining immunofluorescence shows the co-localisation of PU.1/Vimetin in the synovium of patients with RA. (D) IHC staining verifies the upregulation of PU.1 in the hyperplasia joint synovium of CIA mice. (E) IHC staining of the expression levels of FLT3 and p-FLT3 in the joint synovium of healthy donors and patients with OA and RA. (F) Western blotting results of FLT3 and p-FLT3 expression in joint synovium of patients with OA and RA. CIA, collagen-induced arthritis; FLT3, FMS-like tyrosine kinase 3; IHC, immunohistochemical; OA, osteoarthritis; RA, rheumatoid arthritis.

kinase 3 (FLT3) has been demonstrated in RA.[21] Both IHC and western blotting results show that the expression patterns of FLT3 and p-FLT3 were opposite to that of PU.1 in RA synovium (figure 1E,F). In summary, these results suggest that PU.1 and FLT3 might regulate the pathogenesis of RA in macrophages and FLS.

PU.1 UREΔ mice exhibits relieved symptoms of collagen antibody-induced arthritis

Next, PU.1 knockdown (UREΔ) mice (online supplemental figure S1) were used to establish a collagen antibody–induced arthritis (CAIA) mouse model (figure 2A and online supplemental figure S2) to study the role of PU.1 in the pathogenesis of arthritis.

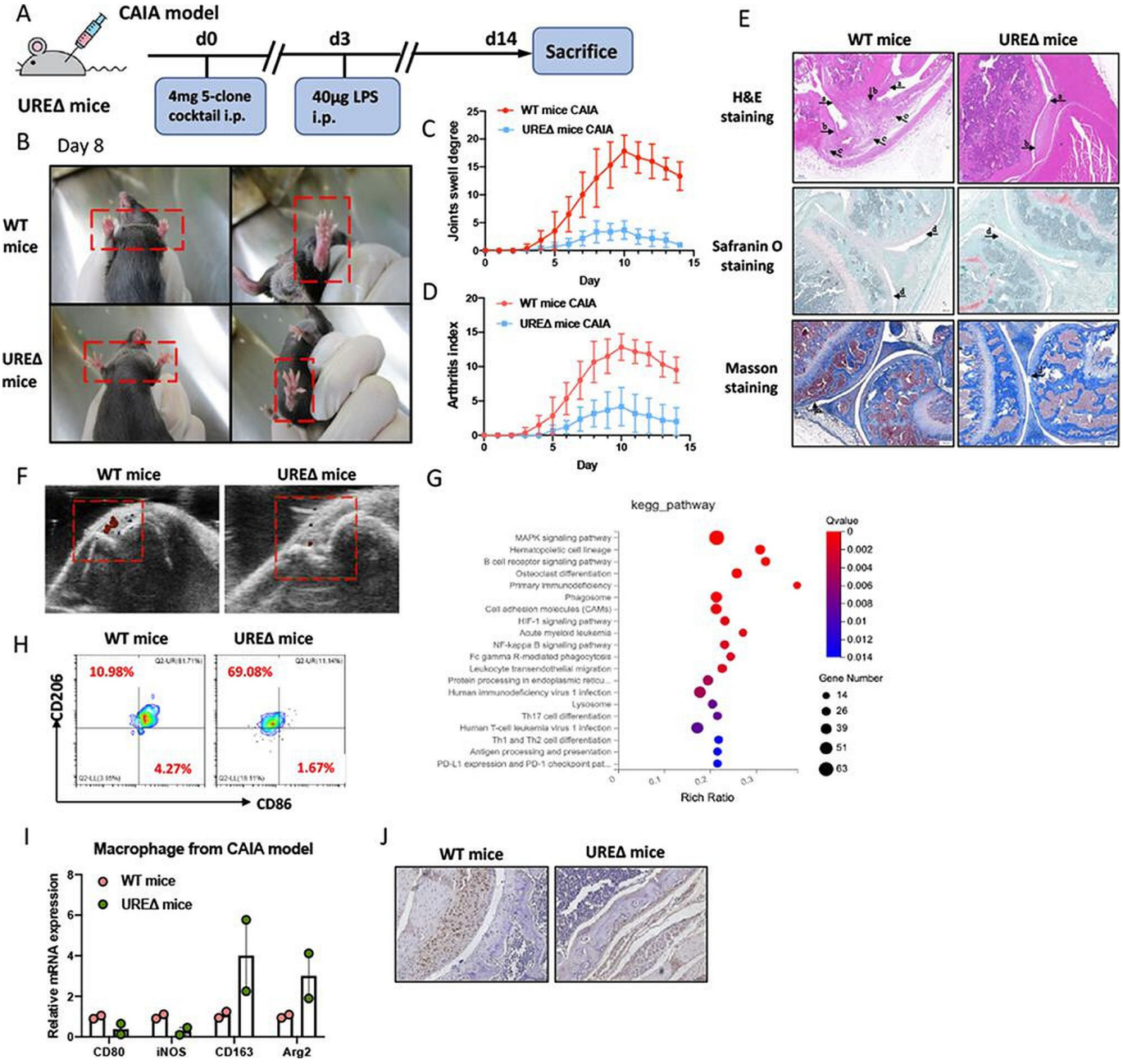

Figure 2 (A) PU.1 knockdown (UREΔ) mice were used to establish a collagen antibody-induced arthritis (CAIA) mouse model. (B) Compared with that of the wild-type (WT) mouse CAIA model, the joint swelling of both fore and hind limbs in the CAIA model of UREΔ mice was relieved. (C, D) The arthritis index and joint swelling number of UREΔ mice were significantly lower than those of WT mice. (E) H&E staining demonstrates that the synovial hyperplasia of UREΔ mice was much lower than that of WT mice. Safranine O and Masson staining indicates that the cartilage destruction and the proliferation of FLS in the joint synovium of CAIA in UREΔ mice were significantly ameliorated compared with those in WT mice. (A) Synovial hyperplasia; (B) inflammatory cell infiltration; (C) pannus formation; (D) cartilage destruction; (E) osteoclastogenesis. (F) Ultrasonic detection signal of blood flow was weaker at the joints of UREΔ mice than those of the WT CAIA mice. (G) RNA-seq results show that PU.1 knockdown was closely associated with various immune cells in PBMC from UREΔ mice-established CAIA model at the transcriptome level. (H, I) The M1 and M2 percentages of peritoneal macrophages also show that the UREΔ mice had a weaker proinflammatory phenotype. (J) IHC staining of the joint synovium shows that the expression of the FLS marker vimentin in the joint synovium of UREΔ mice decreased. Data are presented as mean±SEM. Student's t-test was performed. FLS, fibroblast-like synoviocytes; IHC, immunohistochemical; LPS, lipopolysaccharide.

Compared with that in the wild-type mouse CAIA model, the joint swelling of both the fore and hind limbs in the CAIA model of UREΔ mice was relieved (figure 2B). The arthritis index and joint swelling number of UREΔ mice were significantly lower than those of the wild-type mice (figure 2C,D). In addition, several experimental methods have been used to study pathological changes in the joint synovium of UREΔ mice. H&E staining demonstrated that the synovial hyperplasia of UREΔ mice was much lower than that of wild-type mice (figure 2E). The results of Safranine O and Masson staining indicated that the cartilage destruction and the proliferation of FLS in the joint synovium of CAIA in UREΔ mice were significantly ameliorated than those in wild-type mice (figure 2E). Ultrasonic detection revealed that the blood flow signal was weaker at the joints of UREΔ mice than that of wild-type CAIA mice (figure 2F), suggesting that the pannus formation of CAIA in UREΔ mice was less than that in wild-type mice. In addition, RNA-seq was performed to evaluate the effects of PU.1 knockdown on CAIA model-derived peripheral blood mononuclear cell (PBMC) at the transcriptome level. Results of Kyoto Encyclopaedia of Genes and Genomes (KEGG) pathway analysis showed that various immune cells (such as T cell, B cell and macrophage) and several related immunological pathways were significantly affected in PBMC from the UREΔ mouse-established CAIA model, suggesting that PU.1 knockdown affects CAIA model-derived PBMC at the transcriptome level (figure 2G and online supplemental figure S3). Interestingly, The M1 and M2 percentages of peritoneal macrophages (online supplemental figure S4) show that UREΔ mice had a weaker proinflammatory phenotype (figure 2H). qPCR results of M1 and M2 markers in peritoneal macrophages further validated this point (figure 2I). Finally, IHC staining of the joint synovium showed that the expression of the FLS marker vimentin in the joint synovium of UREΔ mice decreased, consistent with hyperplasia of FLS being weaker in the CAIA of UREΔ mice (figure 2J). Taken together, these results demonstrated that PU.1 knockdown mice exhibited relieved symptoms of CAIA and that macrophage and FLS in PU.1 knockdown mouse CAIA tended to exhibit anti-inflammatory phenotypes.

PU.1 represses FLT3 transcription via directly binding to the FLT3 promoter

It has been reported that FLT3 stop mutations increase the risk of autoimmune diseases including RA.[22] Based on the negative correlation between PU.1 and FLT3,[23] we proposed that PU.1 inhibits FLT3 in RA (figure 3A). To verify this hypothesis, we first measured the expression levels of FLT3 in the CAIA model of UREΔ mice. The results of flow cytometry showed that the endogenous expression of FLT3 in macrophages and FLS in the CAIA model of UREΔ mice was significantly increased (figure 3B–D). To investigate the regulatory effect of the transcriptional factor PU.1 on FLT3 transcription, we cloned the FLT3 promoter region and constructed the pGL-FLT3 plasmid. Under the action of the PU.1 overexpression plasmid, the transcriptional activity of the FLT3 promoter was significantly reduced (figure 3E).

FLT3-ITD mice exhibits relieved symptoms of CAIA

To further verify the role of FLT3 in RA, we used FLT3-ITD mice to construct a CAIA model (figure 4A, online supplemental figures S5 and S6). The *FLT3* gene in FLT3-ITD mice was hyperactivated because of a mutation in the *FLT3* gene. Compared with the CAIA model using the same wild-type littermate, the CAIA model of FLT3-ITD mice had a lower paw swelling number and arthritis index (figure 4B–D). Similar to those of the UREΔ mice, the results of H&E staining and ultrasound assays show that the joint destruction and neovascularisation of the CAIA model of FLT3-ITD mice were weaker than those of the CAIA model of wild-type mice (figure 4E). In addition, Safranin O, Masson and TRAP staining demonstrated that joint fibroblast hyperplasia, cartilage destruction, and osteoclasts reduced in the CAIA model of FLT3-ITD mice (figure 4F), suggesting that FLT3 activation alleviates the severity of arthritis. At the cellular level, peritoneal macrophages of the CAIA model of FLT3-ITD mice showed a less inflammatory phenotype (figure 4G,H). Immunohistochemical staining also showed that the proliferation of FLS in the joint synovium of the CAIA model of FLT3-ITD mice reduced, as was the number of infiltrated $CD11b^{+}$ macrophages (figure 4I). Taken together, these results demonstrated that FLT3 is an anti-inflammatory factor and that FLT3 activation can prevent the pathogenesis of arthritis.

Effects of the PU.1-FLT3 axis on macrophage and FLS in vitro

To further illustrate the effects of the PU.1-FLT3 axis on several key cellular components in RA, siRNAs were used to knock down the endogenous expression of PU.1 and FLT3 in macrophages and FLS in vitro (online supplemental figure S7). The siRNA-mediated knockdown of PU.1 suppressed inflammatory features of murine macrophage cell line RAW264.7, including the M1/M2 ratio and expression of inflammatory cytokines (figure 5A,B). In addition, primary monocytes were isolated from peripheral blood of RA patients and differentiated to M0 macrophages via stimulation of M-CSF. qPCR results demonstrated that pro-inflammatory markers were upregulated and anti-inflammatory markers were repressed in PU.1 knockdown primary macrophages (figure 5C). Except macrophage, we also investigated the effects of PU.1 knockdown on primary FLS from RA patients (RA-FLS). First, RNA-seq was performed to evaluate the effects of PU.1 knockdown on RA-FLS at the transcriptome level. Results of KEGG pathway analysis showed that various inflammatory associated pathways, including PI3K/AKT, HIF-1, TNF, VEGF signalling pathways, were changed in PU.1 KD RA-FLS, implying that PU.1 knockdown modulates RA-FLS related inflammation (figure 5D and online supplemental figure S8). In addition, the proliferation, migration and expression of inflammatory cytokines were all downregulated in PU.1 knockdown RA-FLS (figure 5E–G). Furthermore, FLT3 siRNA-mediated knockdown (online supplemental figure S9) demonstrated the opposite effects of PU.1 siRNA in both primary mouse macrophages, THP-1 cells-induced macrophages (THP-1-M), monocyte-derived macrophages from RA patients (figure 6A–C, online supplemental figure S10) and RA-FLS (figure 6D–F), suggesting that FLT3 is a functional target of PU.1 in two cellular components in RA. Taken together, our results showed that PU.1-FLT3 is an essential proinflammatory axis in RA that promotes inflammatory features in macrophages and RA-FLS.

Pu.1 inhibitor mitigates arthritis of CAIA and CIA mice

DB2313 is a small molecule that can inhibit the binding of PU.1 to its target genes, thus inhibiting the function of its transcription factors.[24] In this study, DB2313 was administered to two mouse arthritis models, CAIA and CIA mice (online supplemental figures S11 and S12), to further evaluate the effect of directly inhibiting PU.1 function on the progression of arthritis. As expected, DB2313 significantly inhibited the progression of arthritis in CAIA mice (figure 7A,B). Specifically, DB2313 alleviated arthritis index and joint swelling (figure 7C,D), synovial

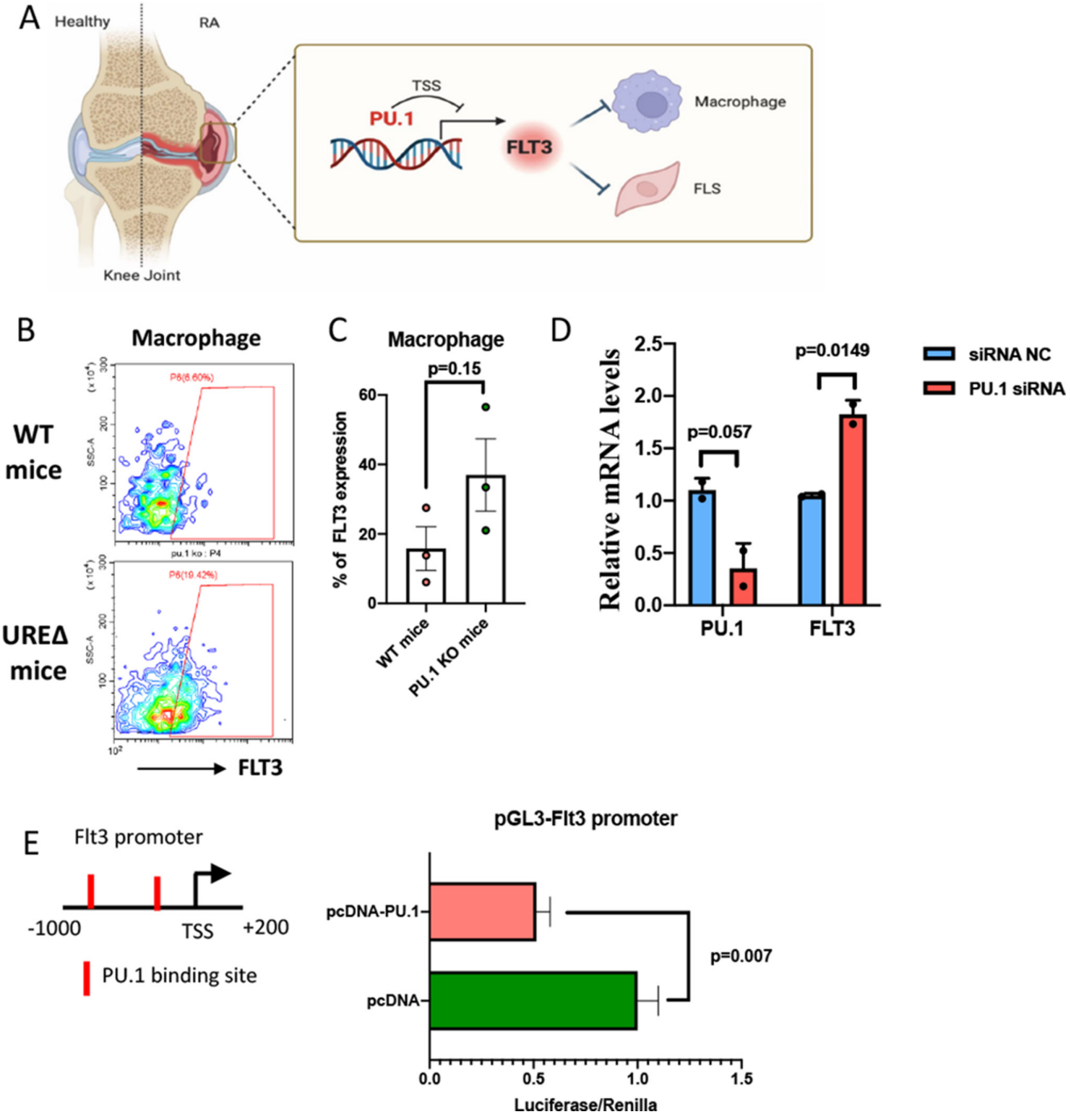

Figure 3 Pu.1 represses FLT3 transcription via directly binding to the FLT3 promoter. (A) PU.1 might inhibit transcription of FLT3 in RA. (B–D) FLT3 expression levels in macrophages and FLS of CAIA model of UREΔ mice. (E) Transcription of the FLT3 promoter was inhibited by PU.1. Data are presented as mean±SEM. Student's t-test was performed. CAIA, collagen antibody-induced arthritis; FLS, fibroblast-like synoviocytes; FLT3, FMS-like tyrosine kinase 3; RA, rheumatoid arthritis.

hyperplasia (figure 7E), pannus formation in the joint synovium (figure 7F), cartilage destruction and osteoclast formation in CAIA mice (figure 7G,H). Consistent with these results, the production of Osteoprotegerin was restored and Receptor activator of NF-kappaB ligand was repressed in the serum of these DB2313-treated mice (online supplemental figure S13). At the cellular level, DB2313 also inhibited the proinflammatory phenotype of peritoneal macrophages (figure 7I). Immunohistochemical results for vimentin also showed that DB2313 inhibited FLS hyperplasia in the CAIA joint synovium (figure 7J).

CIA is another well-established model of arthritis (figure 8A). The overall therapeutic effects of DB2313 were first evaluated in this study, including the joint swelling degree (figure 8B) and arthritis index (figure 8C). The swelling morphology of the fore and rear paws of CIA mice was also ameliorated by DB2313 treatment (figure 8D). In addition, pannus formation in the joint synovium was also repressed in the DB2313 group compared with that in the vehicle group (figure 8E). MicroCT results demonstrated that DB2313 alleviated arthritis-induced bone damage (figure 8F). H&E, Masson, Safranin O and TRAP staining results showed that DB2313 alleviated synovial hyperplasia, cartilage destruction, and osteoclast formation in the CIA model (figure 8G). In addition, peritoneal macrophages showed an anti-inflammatory phenotype in the DB2313 group (figure 8H). The immunohistochemical analysis of CD11b and vimentin confirmed that DB2313 repressed the infiltration of macrophages and hyperplasia of FLS in the CAIA joint synovium (figure 8I). Our results showed that the PU.1 inhibitor DB2313 significantly repressed arthritis development in the two arthritis models, CAIA and CIA.

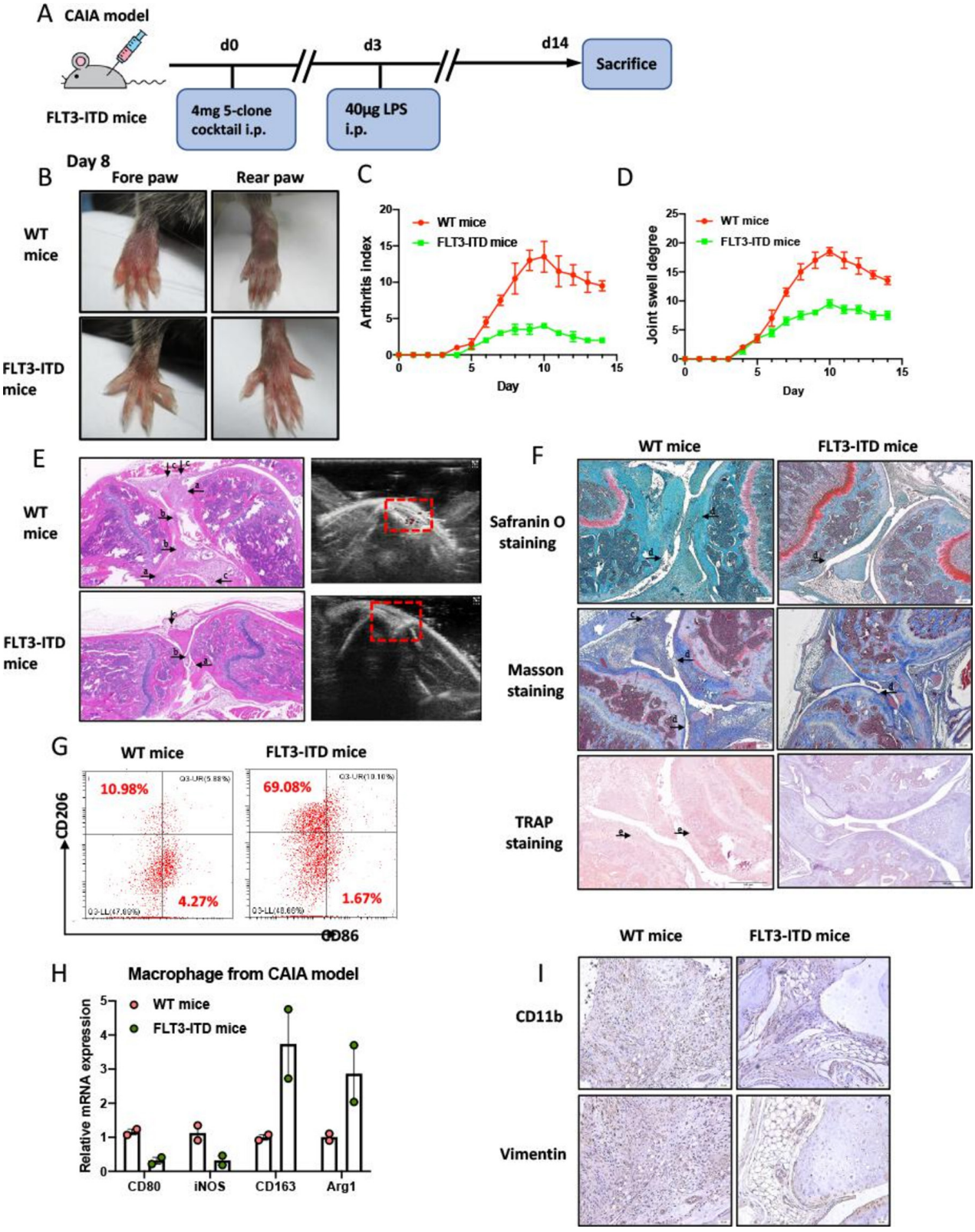

Figure 4 FLT3-ITD mice exhibits relieved symptoms of CAIA. (A) FLT3-ITD mice were used to construct the CAIA models. (B–D) Compared with the CAIA model using the same wild-type littermate, the CAIA model of FLT3-ITD mice had lower paw swelling number and arthritis index. (E, F) H&E staining and ultrasound assays show that the joint destruction and neovascularisation of the CAIA model of FLT3-ITD mice were smaller than those of the CAIA model of wild-type mice. (F) Safranin O, Masson and TRAP staining demonstrate that the joint fibroblast hyperplasia, cartilage destruction and osteoclasts were reduced in the CAIA model of FLT3-ITD mice. (A) Synovial hyperplasia; (B) inflammatory cell infiltration; (C) pannus formation; (D) cartilage destruction; (E) osteoclastogenesis. (G, H) The peritoneal macrophages of the CAIA model of FLT3-ITD mice all showed a less inflammatory phenotype. (I) Immunohistochemical staining demonstrates and the number of infiltrated $CD11b^{+}$ macrophages and vimentin+FLS are also decreased. Data are presented as mean±SEM. Student's t-test was performed. CAIA, collagen antibody-induced arthritis; FLS, fibroblast-like synoviocytes; FLT3, FMS-like tyrosine kinase 3; WT, wild-type.

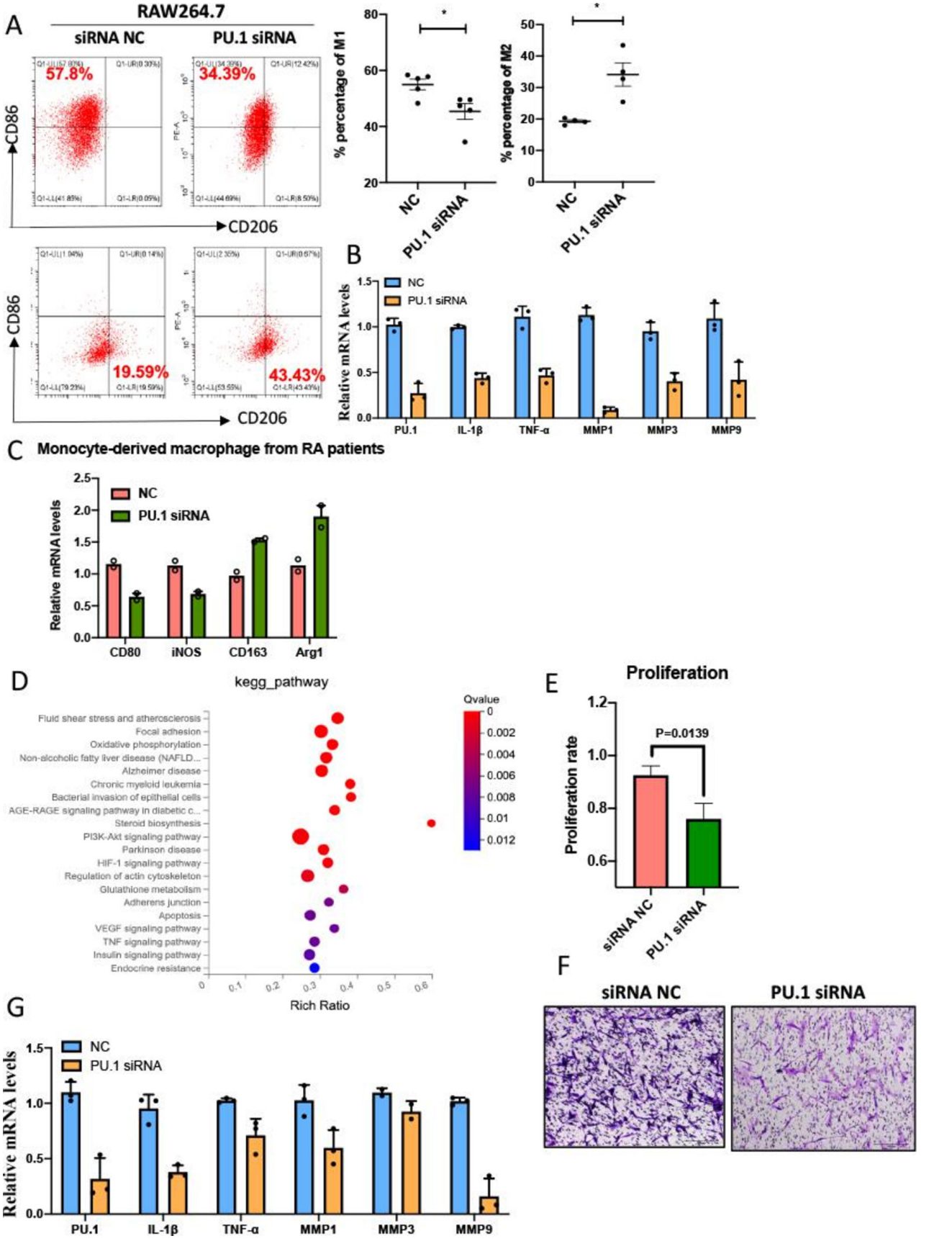

Figure 5 Effects of the PU.1 on macrophage and FLS in vitro. (A–C) The siRNA-mediated knockdown of PU.1 suppresses inflammatory features of murine macrophage cell ine RAW264.7 and primary macrophages, including the M1/M2 ratio and expression of inflammatory cytokines, which are also repressed by PU.1 siRNA. (D) RNA-seq results of the effects of PU.1 knockdown on RA-FLS at the transcriptome level. (E–G) The proliferation, migration and expression of inflammatory cytokines are downregulated in PU.1 knockdown RA-FLS. Data are presented as mean±SEM. Student's t-test was performed. FLS, fibroblast-like synoviocytes; RA, rheumatoid arthritis.

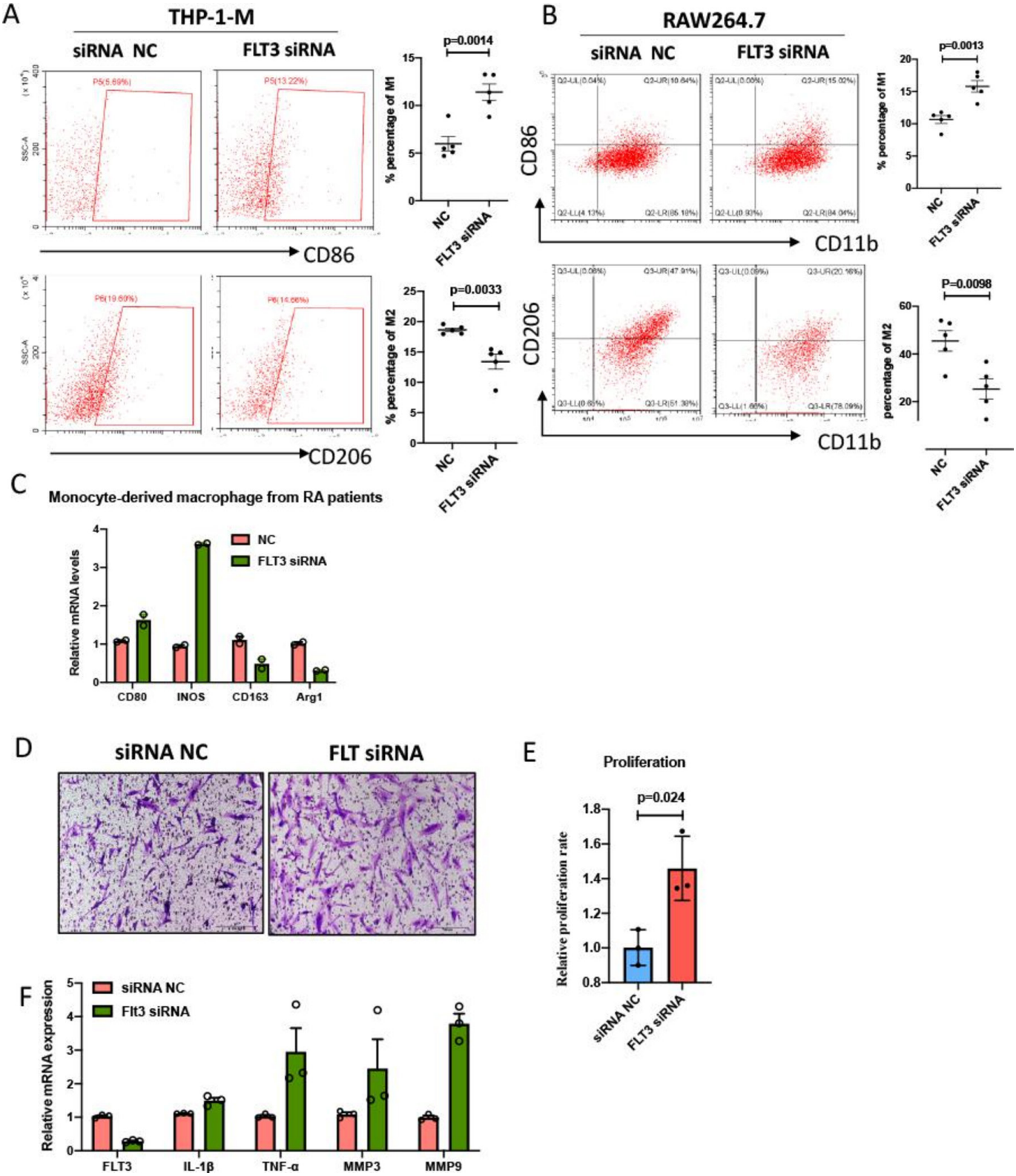

Figure 6 Effects of the FLT3 on macrophage and FLS in vitro. (A–C) FLT3 siRNA-mediated knockdown demonstrates the opposite effects of PU.1 siRNA in THP-1-M and RAW264.7. (D–F) The proliferation, migration and expression of inflammatory cytokines are induced in FLT3 knockdown RA-FLS. Data are presented as mean±SEM. Student's t-test was performed. FLS, fibroblast-like synoviocytes; FLT3, FMS-like tyrosine kinase 3; RA, rheumatoid arthritis.

DISCUSSION

PU.1, a key transcription factor, is involved in the differentiation of a variety of immune cells, and its role in immune cell-associated tumours has been extensively studied.[20] Although its key role in immune cells is known, the specific function of PU.1 in autoimmune diseases remains unclear. RA is an autoimmune disease with the highest incidence and most extensive impact worldwide. Its main pathogenesis is closely related to the abnormal

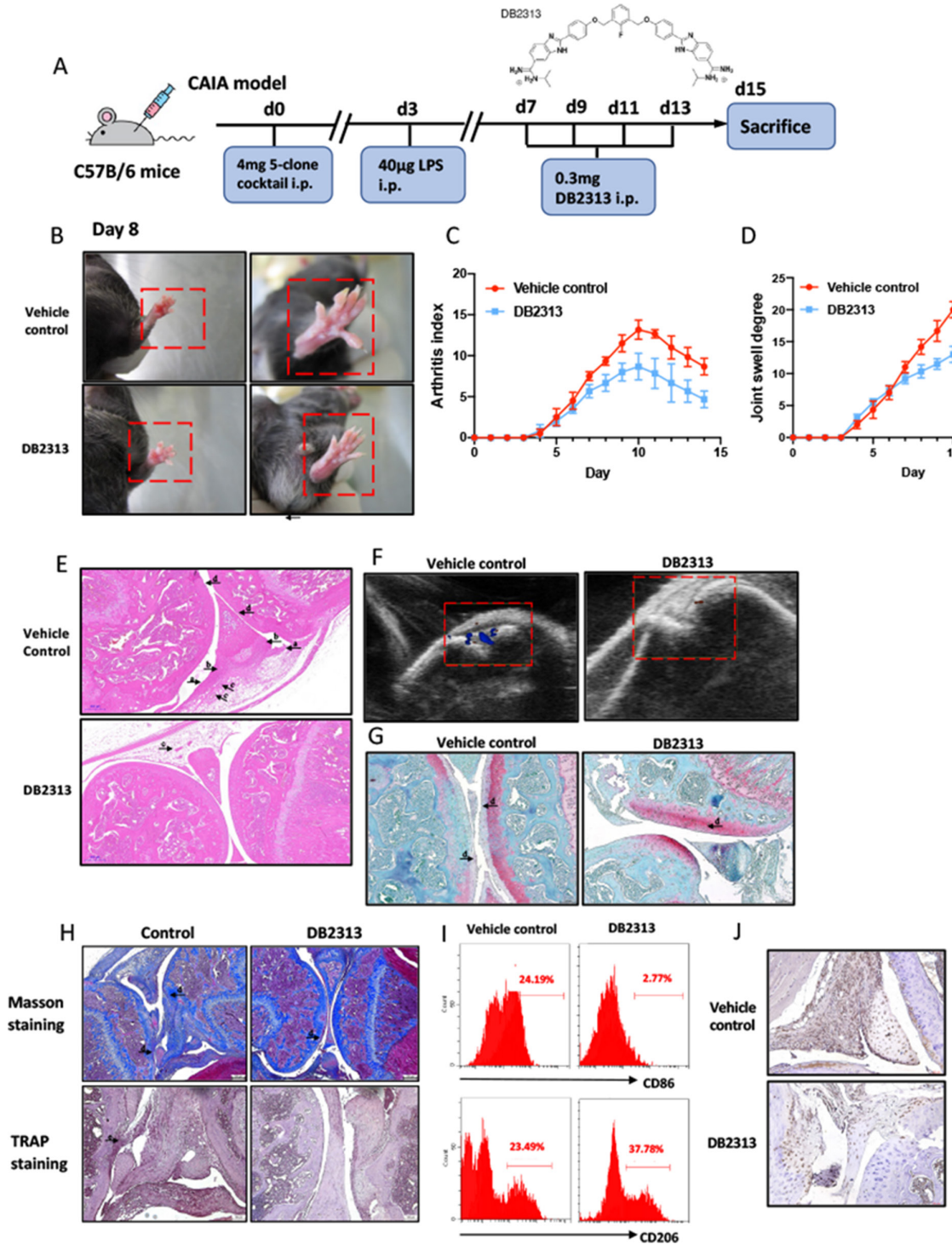

Figure 7 Pu.1 inhibitor mitigates arthritis of CAIA mice. (A) DB2313 is given to collagen and antibody-induced arthritis (CAIA) to evaluate the effect of directly inhibiting PU.1 function on the progression of arthritis. (B) DB2313 significantly inhibits the progression of arthritis in CAIA mice. (C) DB2313 alleviates arthritis index and joint swelling. (E, F) DB2313 alleviates synovial hyperplasia and Pannus formation in the joint synovium. (G, H) DB2313 alleviates cartilage destruction and osteoclast formation in CAIA mice. (I) At the cellular level, DB2313 inhibits the pro-inflammatory phenotypes of peritoneal macrophages of CAIA mice. (J) Immunohistochemical results of vimentin shows that DB2313 inhibit the hyperplasia of FLS in the CAIA joint synovium. Data are presented as mean±SEM from at least 6 mice per group. Student's t-test was performed. FLS, fibroblast-like synoviocytes.

activation of a variety of immune cells such as macrophages, T cells, B cells and neutrophils. Synovitis, one of the main pathological manifestations of RA, is also closely associated with the hyperproliferation and invasion of FLS in the joint synovium. Based on the important regulatory role of PU.1 in a variety of immune cells under both physiological and pathological states, the essential roles of various immune cells in RA, combined with previous literature research and our preliminary experimental results, we hypothesised that PU.1 might play an important role in the pathogenesis of RA. In this study, we demonstrated that

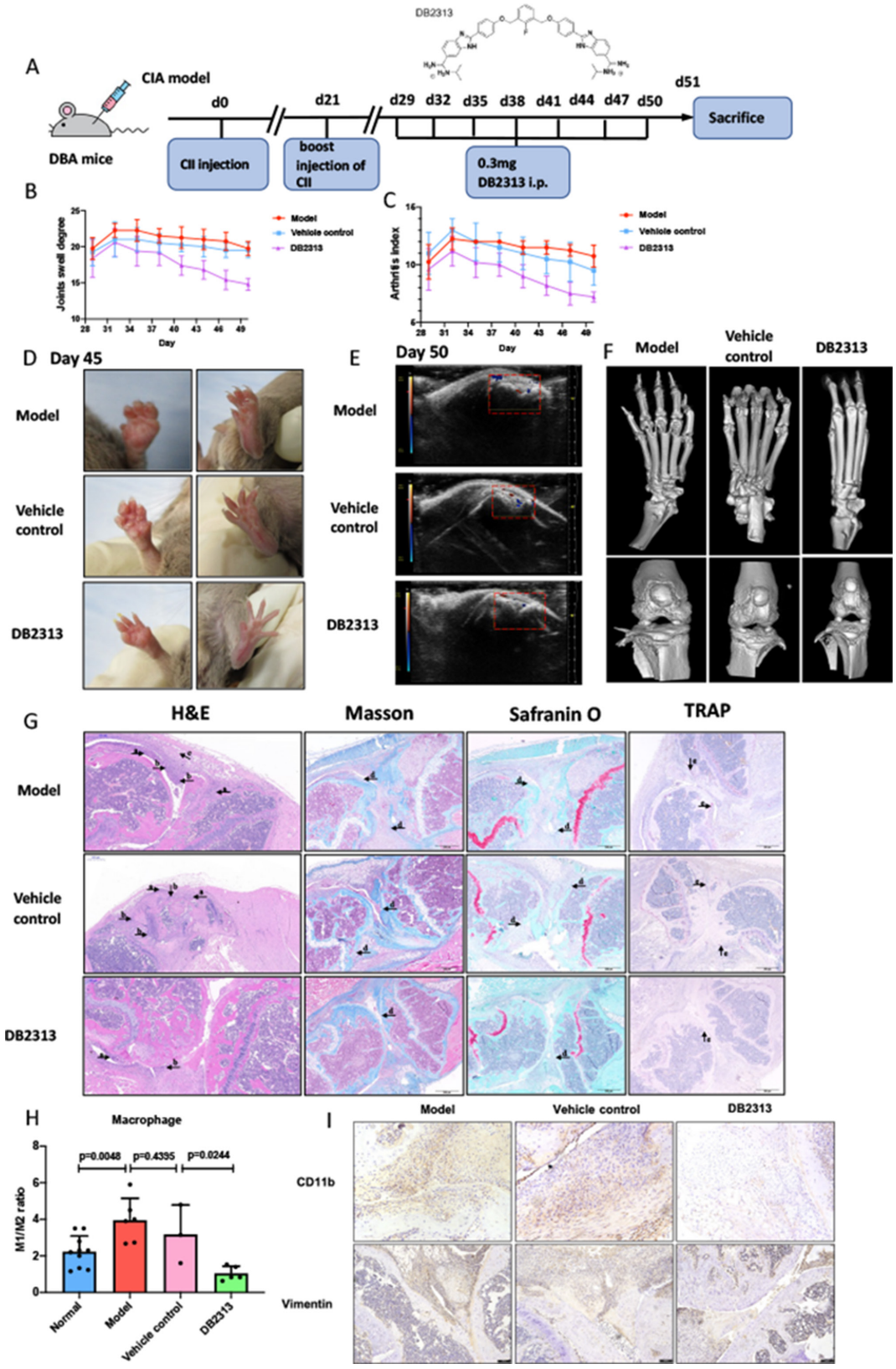

Figure 8 Pu.1 inhibitor mitigates arthritis of CIA mice. (A) DB2313 was given to collagen-induced arthritis (CIA). (B, C) DB2313 significantly inhibits the index of joint swelling and arthritis index of CIA mice. (D) DB2313 significantly inhibits the joint swelling of CIA mice. (E) DB2313 alleviates Pannus formation in the joint synovium of CIA mice. (F) DB2313 alleviates bone destruction of CIA mice. (G) H&E staining shows that DB2313 significantly inhibits the overall pathogenic destruction in the joint of CIA mice. Masson and safranin O staining demonstrate that DB2313 significantly represses destruction of bone and cartilage the in the joint of CIA mice. Trap staining suggests that DB2313 inhibits osteoclast differentiation in the joint of CIA mice. (H) At the cellular level, DB2313 inhibits the proinflammatory phenotypes of peritoneal macrophages in CIA mice. (I) mmunohistochemical results of vimentin shows that DB2313 inhibit the hyperplasia of FLS and infiltration of macrophages in the CIA joint synovium. Data are presented as mean±SEM. Student's t-test was performed. FLS, fibroblast-like synoviocytes.

PU.1 simultaneously affected the proinflammatory response of two types of cellular components in RA: (1) PU.1 induces the proinflammatory features of macrophages by inducing the M1/M2 ratio and the expression of various inflammatory factors and MMPs; and (2) PU.1 can activate the malignant characteristics of RA-FLS in the joint synovium by promoting its hyperproliferation and invasion and the production of proinflammatory factors and MMPs, showing the promotive effects of PU.1 on RA regarding synovitis.

FLT3 mutations are one of the important carcinogenic mechanisms of neutrophil and T-cell cancer.[25 26] Similar to PU.1, previous studies of FLT3 have mainly focused on immune cell-associated cancers. However, in recent years, its role in the normal development of a variety of immune cells, such as DC and NK cells, have been reported.[27 28] Based on the role of FLT3 in a variety of immune cells under both physiological (cell development) and pathological conditions (cancer), FLT3 seems to act as a general regulator that affects the function of a variety of immune cells. We predicted that FLT3 may be a direct transcriptional target of PU.1 via bioinformatics, and we have confirmed this regulatory mechanism by showing that PU.1 directly inhibits the transcription of FLT3. In terms of functional experiments, the CAIA model was established using FLT3-ITD mice to confirm that the overexpression of FLT3 inhibited the development of arthritis, and in vitro experiments confirmed that FLT3 exerted its anti-inflammatory effect in macrophages and RA-FLS. These results indicated that FLT3 inhibits the development of arthritis as a negative functional downstream target of PU.1.

Regarding the limitations of this study, we believe that there are also future research directions that we need to investigate. (1) Macrophages (LysM-cre) specifically knockout PU.1 and FLT3 mice have been established, specifically with PU.1 knockout, and FLT3 in macrophages could provide a better mouse model to evaluate the effect of the PU.1–FLT3 axis on macrophages in the pathogenesis of mouse arthritis. In this way, we can further determine which cellular component of the PU.1–FLT3 axis plays a major role. (2) We will include more patients and culture the primary synovial macrophages from patients with RA in vitro to evaluate the effect of the PU.1–FLT3 axis. Therefore, we can evaluate whether the promotive effect of PU.1–FLT3 on RA is conserved between humans and mice. (3) We will further illuminate the overall changes of all cell types in the joint synovium in arthritis models using the above-mentioned mice via single-cell sequencing to evaluate the effect of the PU.1–FLT3 axis and provide more insights from the single-cell analysis.

In this study, we reported for the first time that the PU.1–FLT3 axis participates in the development of RA by simultaneously affecting multiple cells. The application of a variety of arthritis models and related experiments of primary cells derived from the joint synovium of patients with RA have confirmed that PU.1 is a key transcriptional factor that promotes the development of this disease, and a series of experiments were also performed to identify whether FLT3 acts as a direct PU.1 target gene and mediates the function of PU.1 in RA. In summary, the PU.1-FLT3 axis is a proinflammatory pathway that may provide potential targets for the treatment of RA. We plan to develop related therapeutic drugs for RA in the future.

MATERIALS AND METHODS

Patients and normal volunteers

The diagnostic criteria for patients with RA adopted the classification criteria from the American College of Rheumatology and the European Alliance of Associations for Rheumatology in 2010. The diagnostic criteria for OA refer to the bone and joint diagnosis and treatment guidelines updated by the Orthopedic Branch of the Chinese Medical Association in 2018. Human knee synovial tissues used in this study were obtained from patients with RA and OA who underwent knee arthroplasty. The normal synovial tissues were obtained from knee operations with non-inflammatory knee joint diseases were used as normal controls. Blood samples were obtained from patients with RA and from normal controls.

Animal

UREΔ mice (Spi1tm1.3Dgt/J, JAX Strain #: 006083) and FLT3-ITD mice (B6.129-Flt3tm1Dgg/J, JAX Strain #: 011112) were purchased from Jackson lab (USA). DBA/1JGpt mice were purchased from GemPharmatech. This study was approved by the Ethics Committee of Institute of Clinical Pharmacology of Anhui Medical University (PZ-2021-025).

Primary mouse macrophage isolation

Mice are sterilised with 75% ethanol after sacrifice. Then inject 5 mL precooled PBS intraperitoneally and gently massage the abdomen for 5 min; aspirate the PBS in the abdominal cavity into a 15 mL centrifuge tube and place it on ice; centrifugation (300 g, 10 min) and discard supernatant, add 10% DMEM medium to resuspend cell palate and seed cells into 12-well plate, change medium after 4 hours. The purity of adherent macrophage is validated by CD11b and F4/80 staining.

CAIA model

On day 0, an intraperitoneal injection of 4 mg of 5-clonal collagen antibody mixture was administered and, on day 3, an intraperitoneal injection of 40 μg LPS. The control group was administered the same volume of normal saline, and the number of joint swelling and arthritis index were observed and recorded every day after injection. On day 14, the mice were euthanised with an anaesthetic. The scoring criteria for the number of joint swelling: ankle and toe joints are counted and each joint swelling is one point. The maximum number of joint swelling is 22 points per mouse.

The scoring criteria for arthritis index: 2 independent blind observers scored the arthritis index of mice daily. The scoring standard is 0–4 different grades: 0 points, no local redness and swelling; 1 point, the phenomenon of swelling of the knuckles appears; 2 points, there is a slight swelling of the ankle or wrist joint; For 3 min, the whole foot and claw appear severely swollen; 4 min, the claws appear stiff or deformed.

CIA model

Chick type II collagen was sufficiently dissolved in 5 mL of acetic acid (0.1 M), followed by emulsification with complete Freund's adjuvant. On day 0, the mice were intradermally injected with 0.15 mL CII emulsion. On day 21, the mice were restimulated by intradermal injection of 0.1 mL CII emulsion.[29] On day 29, the success rate of the CIA model was 95%, and the failed models were excluded. Mice were divided into three groups. After the onset of joint swelling on day 29, the mice were treated intraperitoneally. CIA model mice were treated with an equal volume of vehicle. On day 50, the mice were euthanised, and blood, spleen and ankle joints were collected for subsequent studies. The scoring criteria for the number of joint swelling and arthritis index were same as that of CAIA model.

IHC staining

On the 14th day after CAIA modelling and the 50th day after CIA modelling, mice were euthanised with an overdose of anaesthetic. After fixation and decalcification, the knee joint was dehydrated with gradient alcohol, embedded in paraffin and sectioned at 5 µm slices. Tissue sections were then placed into an oven at 60 °C for 2 hours, deparaffinised and hydrated by gradient ethanol, washed with PBS three times, permeabilised for 15 min, washed with PBS three times, antigen repairing for 15 min, washed with PBS three times, blocked with endogenous peroxidase for 10 min, rinsed with PBS for three times and blocked with serum for 15 min. Then, the primary antibodies (anti-human PU.1 (Abcam, ab230336, 1:200), anti-human FLT3 (Affinity Biosciences, DF8546, 1:200), anti-human p-FLT3 (Affinity Biosciences, AF8152, 1:400), anti-CD11b antibody (Abcam, ab133357, 1:400) and anti-human vimentin (Abcam, ab137321, 1:400)) were added, and the mixture incubated overnight at 4°C. The next day, after incubation with biotin-labelled secondary antibody for 20 min at room temperature, the sections were rinsed with PBS three times, horseradish enzyme marker was added dropwise to streptavidin working solution, rinsed with PBS three times, developed colour with DBA, stained with haematoxylin, dehydrated by gradient alcohol and mounted with neutral gum. Finally, the tissue-staining results were observed under an optical microscope.

Immunofluorescence

After blocking with serum for 15 min, the primary antibodies (anti-mouse PU.1 (Abcam, ab230336, 1:50), anti-mouse vimentin (Abcam, ab137321, 1:100), and anti-CD68 antibody (Abcam, ab213363, 1:100)) were added, and the mixture was incubated overnight at 4°C.

Western blotting

An appropriate amount of ground cells or tissue were added to tissue lysate (10 times volume), homogenised, lysed on ice, and centrifuged at 4°C, 12 000 rpm for 10 min. The supernatant was collected and the protein concentration determined with the BCA method. Next, SDS-PAGE was performed to separate total protein. The gel was then transferred to PVDF membranes and blocked with serum for 1 hour. Afterward, the corresponding primary antibodies (anti-human PU.1 (Abcam, ab230336, 1:1000), anti-human FLT3 (Affinity Biosciences, DF8546, 1:1000), and anti-human p-FLT3 (Affinity Biosciences, AF8152, 1:1000)) were added, and the mixture was incubated overnight at 4°C. The membranes were washed with TBST three times; the secondary antibody was added, incubated at room temperature for 1 hour, washed three times with TBST, and developed. Image software was used to analyse the grey value of each band, and the control protein was used to normalise the grey values of the target protein for statistical analysis.

H&E staining

The sections were deparaffinised and hydrated with gradient alcohol, stained with H&E, dehydrated with gradient alcohol and sealed with neutral gum. Histopathological changes were observed and recorded using an optical microscope.

MicroCT

Mouse hindlimbs from different group (CAIA model group, vehicle control group and DB2313 group) were analysed with a microCT system (NEMO, NMC-100). Briefly, the samples were placed in the holder and scanned under the following conditions: scan resolution 7.5 um, supply voltage 90kV, current 0.06mA, the scan progress was done by the acquisition software Cruiser and analysed by analysis software Avatar (V.1.6.5.3).

Masson staining

The paraffin sections were deparaffinised and stained with Weigert iron haematoxylin for 5 min, differentiated with acidic acetic acid, stained with Masson solution, washed with distilled water for 1 min, stained with Ponceau red magenta staining solution for 6 min, washed with acid solution for 1 min, with phosphomolybdic acid solution for 1 min, and with acid solution for 1 min, stained with aniline blue dye solution for 1 min, washed with acid solution for 1 min, discoloured with xylene, and mounted with neutral gum.

Safranin O staining

After deparaffinisation, sections were immersed in Safranin O staining solution for 3 min, washed with distilled water for 1 min, immersed in fast green staining solution for 2 min, washed with distilled water for 1 min, differentiated with 1% glacial acetic acid for 1 min, dehydrated with 95% ethanol, and discoloured with xylene. Finally, the morphological changes in the sections were observed after mounting with neutral gum.

TRAP staining

The substrate solution was prepared according to the instructions and placed onto a 37 °C water bath for 10 min. Then, the cells were mixed with the substrate solution, incubated for 1 hour, and counterstained with haematoxylin for 2–3 min. Then, pictures were obtained after mounting with neutral gum. The positive staining was dark red in the cytoplasm and blue-purple in the nucleus.

FACS

After centrifugation and washing with PBS, surface flow cytometry antibodies were added according to the manufacturer's instructions [anti-mouse CD11b (Biolegend, 101236), anti-mouse F4/80 (Biolegend, 353283), anti-human CD86 (Biolegend, 327702)], and incubated at 4°C in the dark for 30 min, then centrifuged the cells at 1500 rpm for 5 min.

Intracellular staining was added with 100 µL fixative solution at 4°C for 10 min, centrifuged at 1500 rpm for 5 min, discarded supernatant, then added 100 µL cell lysis buffer, and incubated at 4°C for 10 min. After washing with PBS, antibodies (anti-mouse CD68 (Biolegend, 333815), anti-mouse CD206 (Miltenyi Biotec, 130-102-604), anti-mouse FLT3 (Biolegend, 135310), anti-human CD68 (Biolegend, 333815) and anti-human CD206 (Biolegend, 354997)) were added and incubated in the dark at 4°C for 30 min. The cells were centrifuged at 1500 rpm for 5 min to discard unbound antibodies, resuspended in 100 µL PBS and tested by using a flow cytometer (Beckman Coulter, A00-1-1102).

Cell culture and transfection

THP-1 and RAW264.7 cells were cultured in RPMI-1640 medium, and FLS were cultured in DMEM. In addition to the basic medium, a mixture of 10% fetal bovine serum (FBS) and 1% penicillin/streptomycin was added and cultured in a 37°C, 5% CO_2 incubator for routine culturing. For siRNA transfection, the cells were cultured into 6-well plates with basal medium without penicillin/streptomycin for 12 hours. Then, 8 µL siRNA was dissolved into 200 µL OPTI-MEM medium (Gibco), and 6 µL lipofectamine IMAX was dissolved in 200 µL

OPTI-MEM. In the medium, the prepared siRNA and lipofectamine IMAX solutions were mixed in equal volumes and stabilised at room temperature for 15 min. After removal of the cell culture medium, 1600 µL of fresh medium and 400 µL prepared siRNA transfection mixture were added to each well and the cells incubated in a cell incubator for 6 hours. The transfection medium was then replaced by normal medium and the cells were incubated for 48 hours and then used in subsequent experiments.

Transwell assay

A 24-well chamber (8 µm) was used for Transwell assays. Briefly, RA-FLS were resuspended in a serum-free medium, seeded in the upper chamber at 5×10^3 cells/well, and cultured at 37°C and 5% CO_2 for 24 hours. A complete medium containing 10% FBS was added to the lower chamber. After 24 hours, the remaining cells in the upper chamber were gently removed. The migrated cells on the underside of the membrane were fixed with methanol, stained with 0.1% crystal violet, and counted in five random areas of each well under a microscope.

RT-qPCR

TRIzol was used to extract total RNA from cells or tissues and determine its concentration and purity. Samples of qualified purity were used to perform reverse transcription and PCR amplification tests in accordance with the manufacturer's instructions. The PCR reaction volume was 20 µL, and the amplification conditions were predenaturation 95°C, 5 min; cycle (40 times) 95°C, 10 s; 60°C, 35 s; and melting curve 95°C, 15 s; 60°C, 60 s; and 95°C, 15 s. The *GAPDH* gene was used as an internal reference, and the relative quantitative analysis of gene expression was performed using the $2^{-\Delta\Delta CT}$ method.

CCK-8 assay

After proper treatment, a 5×10^5/mL cell suspension (100 µL per well) was added to a 96-well plate, three replicate wells in each group; 10 µL of CCK-8 solution was added, and the plate was incubated for 3 hours. The absorbance was measured at 450 nm using a microplate reader at 3 hours.

RNA-seq

PBMC samples from CAIA mice and primary human RA-FLS were analysed by high-throughput transcriptome sequencing using BGI (Shenzhen, China) to screen for abnormally and specifically expressed genes. A KEGG pathway analysis was performed to estimate the functions of the dysregulated genes in CAIA mice and RA-FLS. The sequencing and analysing processes were performed according to standard protocol of RNA-seq from BGI.[30 31]

Statistical analysis

GraphPad PRISM V.8.2.1 (GraphPad, USA) was used for statistical analysis. Data in figures are shown as the means±SD. One-way or two-way analysis of variance, Student's t-tests and rank sum tests were used to determine the differences between experimental groups. A $p<0.05$ was considered significant.

Correction notice This article has been corrected since it published Online First. The corresponding author has been changed.

Acknowledgements We thank the staff at BGI for performing RNA sequencing and data analyzing. We thank Dr Chen Zhu and Dr Xinming Wang for collecting patient samples and the healthy control volunteers who participated in this study. We also thank the affected patients and healthy volunteers in this study.

Collaborators Dr Chen Zhu, Dr Xinming Wang, Dr Wenming Hong and Dr Zhenbao Li

Contributors JT and WW conceived the project. WC, YF, DH, YC, HJ, ZX, XW, HW and XZ laboratory and animal experiments. WH, ZL, CZ and XW revised the manuscript. All authors approved the final version for submission. WW acts as guarantor for this work.

Funding This study was supported by the National Natural Science Foundation of China (31900616, 81673444, 82003795), the Project of Improvement of Scientific Ability of Anhui Medical University(2020xkjT009), Natural Science Foundation of Anhui Province for young scholars (1908085QH379) and The Open Fund of Key Laboratory of Anti-inflammatory and Immune Medicine, Ministry of Education, P.R. China (Anhui Medical University, KFJJ-2020-01).

Competing interests None declared.

Patient and public involvement Patients and/or the public were not involved in the design, or conduct, or reporting, or dissemination plans of this research.

Patient consent for publication Not applicable.

Ethics approval This study involves human participants and was approved by the Ethics Committee of Anhui Medical University (PJ2021-14-33).

Provenance and peer review Not commissioned; externally peer reviewed.

Data availability statement Data are available on reasonable request.

ORCID iDs
Jiajie Tu http://orcid.org/0000-0002-3895-3726
Wei Wei http://orcid.org/0000-0002-3117-9598

REFERENCES

1 Silvagni E, Sakellariou G, Bortoluzzi A, *et al*. One year in review 2021: novelties in the treatment of rheumatoid arthritis. *Clin Exp Rheumatol* 2021;39:705–20.
2 Tu J, Hong W, Zhang P, *et al*. Ontology and function of fibroblast-like and macrophage-like synoviocytes: how do they talk to each other and can they be targeted for rheumatoid arthritis therapy? *Front Immunol* 2018;9:1467.
3 Tu J, Huang W, Zhang W, *et al*. A tale of two immune cells in rheumatoid arthritis: the crosstalk between macrophages and T cells in the synovium. *Front Immunol* 2021;12:655477.
4 Weyand CM, Goronzy JJ. T-cell-targeted therapies in rheumatoid arthritis. *Nat Clin Pract Rheumatol* 2006;2:201–10.
5 Lee DSW, Rojas OL, Gommerman JL. B cell depletion therapies in autoimmune disease: advances and mechanistic insights. *Nat Rev Drug Discov* 2021;20:79–199.
6 O'Neil LJ, Kaplan MJ. Neutrophils in rheumatoid arthritis: breaking immune tolerance and Fueling disease. *Trends Mol Med* 2019;25:215–27.
7 Tu J, Wang X, Gong X, *et al*. Synovial macrophages in rheumatoid arthritis: the past, present, and future. *Mediators Inflamm* 2020;2020:1–8.
8 Yap H-Y, Tee SZ-Y, Wong MM-T, *et al*. Pathogenic role of immune cells in rheumatoid arthritis: implications in clinical treatment and biomarker development. *Cells* 2018;7:161–19.
9 Edilova MI, Akram A, Abdul-Sater AA. Innate immunity drives pathogenesis of rheumatoid arthritis. *Biomed J* 2021;44:172–82.
10 Croft AP, Campos J, Jansen K, *et al*. Distinct fibroblast subsets drive inflammation and damage in arthritis. *Nature* 2019;570:246–51.
11 Bottini N, Firestein GS. Duality of fibroblast-like synoviocytes in RA: passive responders and imprinted aggressors. *Nat Rev Rheumatol* 2013;9:24–33.
12 Bustamante MF, Garcia-Carbonell R, Whisenant KD, *et al*. Fibroblast-Like synoviocyte metabolism in the pathogenesis of rheumatoid arthritis. *Arthritis Res Ther* 2017;19:1–12.

13 J Malemud C. Chondrocyte apoptosis in rheumatoid arthritis: is preventive therapy possible? *Immunotherapy* 2016;01:102.
14 Tseng C-C, Chen Y-J, Chang W-A, *et al*. Dual role of chondrocytes in rheumatoid arthritis: the chicken and the egg. *Int J Mol Sci* 2020;21:1071.
15 Paulin F, Doyle TJ, Fletcher EA, *et al*. Rheumatoid arthritis-associated interstitial lung disease and idiopathic pulmonary fibrosis: shared mechanistic and phenotypic traits suggest overlapping disease mechanisms. *Rev Invest Clin* 2015;67:280–6.
16 Wu C, Lin H, Zhang X. Inhibitory effects of pirfenidone on fibroblast to myofibroblast transition in rheumatoid arthritis-associated interstitial lung disease via the downregulation of activating transcription factor 3 (ATF3). *Int Immunopharmacol* 2019;74:105700.
17 Hosokawa H, Rothenberg EV. How transcription factors drive choice of the T cell fate. *Nat Rev Immunol* 2021;21:162–76.
18 Turkistany SA, DeKoter RP. The transcription factor PU.1 is a critical regulator of cellular communication in the immune system. *Arch Immunol Ther Exp* 2011;59:431–40.
19 Solomon LA, Podder S, He J, *et al*. Coordination of myeloid differentiation with reduced cell cycle progression by PU.1 induction of microRNAs targeting cell cycle regulators and lipid anabolism. *Mol Cell Biol* 2017;37:e00013–17.
20 Burda P, Laslo P, Stopka T. The role of PU.1 and GATA-1 transcription factors during normal and leukemogenic hematopoiesis. *Leukemia* 2010;24:1249–57.
21 Gebru MT, Wang H-G. Therapeutic targeting of FLT3 and associated drug resistance in acute myeloid leukemia. *J Hematol Oncol* 2020;13:155.
22 Saevarsdottir S, Olafsdottir TA, Ivarsdottir EV, *et al*. FLT3 stop mutation increases FLT3 ligand level and risk of autoimmune thyroid disease. *Nature* 2020;584:619–23.
23 Inomata M, Takahashi S, Harigae H, *et al*. Inverse correlation between Flt3 and PU.1 expression in acute myeloblastic leukemias. *Leuk Res* 2006;30:659–64.
24 Antony-Debré I, Paul A, Leite J, *et al*. Pharmacological inhibition of the transcription factor PU.1 in leukemia. *J Clin Invest* 2017;127:4297–313.
25 Kennedy VE, Smith CC. *FLT3* Mutations in Acute Myeloid Leukemia: Key Concepts and Emerging Controversies. *Front Oncol* 2020;10:612880.
26 Daver N, Schlenk RF, Russell NH, *et al*. Targeting FLT3 mutations in AML: review of current knowledge and evidence. *Leukemia* 2019;33:299–312.
27 Karsunky H, Merad M, Cozzio A, *et al*. Flt3 ligand regulates dendritic cell development from Flt3+ lymphoid and myeloid-committed progenitors to Flt3+ dendritic cells in vivo. *J Exp Med* 2003;198:305–13.
28 Guimond M, Freud AG, Mao HC, *et al*. In vivo role of FLT3 ligand and dendritic cells in NK cell homeostasis. *J Immunol* 2010;184:2769–75.
29 Chen J, Wang Y, Wu H, *et al*. A modified compound from paeoniflorin, CP-25, suppressed immune responses and synovium inflammation in collagen-induced arthritis mice. *Front Pharmacol* 2018;9:563.
30 Tu J, Huang W, Zhang W, *et al*. TWIST1-MicroRNA-10a-MAP3K7 axis ameliorates synovitis of osteoarthritis in fibroblast-like synoviocytes. *Mol Ther Nucleic Acids* 2020;22:1107–20.
31 Tu J, Han D, Fang Y, *et al*. MicroRNA-10b promotes arthritis development by disrupting $CD4^+$ T cell subtypes. *Mol Ther Nucleic Acids* 2022;27:733–50.